EUROPEAN LABORATORY FOR PARTICLE PHYSICS

CERN-EP/98-094
16th June 1998

Prospects for the Higgs Boson Search in e^+e^- Collisions at LEP 200

E. Gross [1], A. L. Read [2] and D. Lellouch[1].

Abstract

We evaluate the combined sensitivity of the four LEP collaborations to exclude (at the 95% C.L.) or discover (at the 5σ level) the Standard Model Higgs boson with the LEP collider at centre-of mass energies of 189,198 and 200 GeV. It is shown that with 200 pb^{-1} of luminosity collected at a centre-of-mass energy of 198 GeV a Higgs boson of 104.5 (107.0) GeV/c^2 can be discovered (excluded). It is also argued that the Standard Model Higgs search benefits from an upgrade of LEP to its peak centre-of-mass energy (e.g. upgrade 198 GeV to 200 GeV) provided the delivered integrated luminosity exceeds 50% of that obtainable at the lower energy.

Submitted for publication in the proceedings of the Rencontres de Physique de la Vallee' d'Aoste, La Thuile March 1998.

[1]Particle Physics Department, Weziamnn Institute of Science, Rehovot 76100, Israel and the OPAL experiment, CERN.

[2]Physics Department, University of Oslo, Blindern, NO-1000 Oslo 3, Norway and the DELPHI experiment, CERN.

1 Introduction

During 1995 a workshop was held at CERN in order to evaluate the physics prospects of LEP 200[1]. In this workshop the four LEP collaborations, ALEPH, DELPHI, OPAL and L3, cooperated in order to evaluate their combined sensitivity to exclude (at the 95% C.L.) or discover (at the 5σ level) the Standard Model Higgs boson with the LEP collider running at $\sqrt{s}$ = 175, 192 and 205 GeV. More than two years have passed since that report. During these years three subsequent energy upgrades of the LEP collider contributed to the Standard Model Higgs search at LEP 200. Each experiment collected 10 pb^{-1} of luminosity[3] during the summer of 1996 at a centre-of-mass energy of 161 GeV. An additional 10 pb^{-1} were collected the following autumn at a centre-of-mass energy of 172 GeV. Late in the summer of 1997 the centre-of-mass energy was raised to 183 GeV and LEP provided a luminosity of 55 pb^{-1}. Although the Higgs boson has not been discovered yet, the lower bounds put on its mass are more stringent than all predictions of the above mentioned LEP 200 workshop. An important reason that the workshop predictions were exceeded is that the experiments gained valuable experience in dealing with LEP 200 backgrounds (in particular 4-fermion backgrounds like W^+W^- and $\mathrm{Z}^0\mathrm{Z}^0$) based on excellent b-tagging and the replacement of cuts-based analyses with multidimensional likelihood and Neural Network based analyses. Another major improvement since the workshop is the statistical treatment of the search results.

The LEP experiments have learned how to deal with candidate events. Statistical methods were developed in order to cope with candidate events coming from various channels (with varying significance) which have specific masses and non-Gaussian mass distributions. The LEP Working Group for Higgs boson searches has advanced a lot the statistical analyses [2] and all experiments have by now very mature and well-tested statistical procedures.

To be more specific, in the LEP200 workshop [1] the simulated search results were analyzed separately for different centre-of-mass energies, the search was treated as a single-channel counting experiment (candidates selected in a signal poor, background rich channel carried the same weight as those from a signal rich, background poor channel), and the reconstructed invariant masses of the Higgs candidates and the relevant resolution functions were used in a rudimentary fashion (events were selected inside a $\pm 2\sigma$ window around the m_{H^0} hypothesis). In the present study the results at different centre-of-mass energies were combined, the invariant mass information was used more effectively, the search channels were treated individually, and the results combined in an optimal way. Thus a revision of the LEP 200 prospectives study was necessary.

The aim of this study is to estimate the luminosities (at $\sqrt{s}$= 189, 198 and 200 GeV) required to gain the maximal sensitivity for exclusion or discovery of the Higgs boson. While the 1995 workshop examined only the individual cases, we examine combinations of up to three prospective centre-of-mass energies, however, at its peak energy the luminosity that can be delivered by the machine might be lower than the luminosity that can be provided a few GeV

[3] **All luminosities in this paper are per experiment, while the results are given for the combined four experiments.**

below the peak [3]. In this paper we examine as an example, the trade-off between 100 pb^{-1} collected at $\sqrt{s}$=198 GeV and 50 pb^{-1} collected at $\sqrt{s}$=200 GeV.

The fast Monte Carlo which was used to simulate the basic kinematical quantities by which the background is reduced with respect to the Higgs signal is described in Section 2. Basically we have used cuts accompanied by kinematic fits and parametrized b-tagging. The selection analysis is described in Section 3. The statistical procedures are described in Section 4. The derived results are discussed in Section 5. The conclusions are given in Section 6.

2 The fast Monte Carlo

The response of a typical LEP detector was described by the following parameterization (inspired by the OPAL detector): an acceptance of $|\cos\theta| < .98$ is assumed for tracks and calorimetric clusters. The acceptance of the forward detector (luminometer) covers $28 < \theta < 200$ mrad; this device is used only for vetoing on forward energy.

The transverse momentum of charged tracks is measured by the central track-detector with the resolution: $\delta p_T = p_T * \sqrt{\alpha^2 + \beta^2 p_T^2}$, where $\alpha = .01$, $\beta = .00075$, and p_T is expressed in GeV/c. The energy of calorimetric clusters is measured with the resolution $\delta E = 85\% * \sqrt{E}$, where E is expressed in GeV.

In order to simulate the problem of energy double counting of charged particles by the tracking detector and the calorimeters, we estimate energy flows in events by calorimetry measurements only. This is not the case for electrons and muons with $p > 10\,\mathrm{GeV/c}$, which are assumed to be well identified. For these particles, the uncertainty on the energy comes from the momentum resolution of the track detector. Finally, angles are assumed to be measured with infinite precision.

To simulate a b-tagger we implemented the impurity versus efficiency curve shown in Fig. 1. For each jet the number of particles containing a b-flavour quark is required to be bigger than 2. Then one fixes the required efficiency and a random number generator is used in order to determine if the jet is identified as a b-jet or not (via the impurity).

The signal detection efficiencies and accepted background cross-sections are estimated using Monte Carlo samples processed through the fast detector simulation. The HZHA generator [4] is used to simulate Higgs boson production processes (both the Bjorken and the fusion processes). The generated partons are hadronised using JETSET [6]. The background processes are generated using the Pythia event generator [6].

3 The Analysis

At LEP 200 the Standard Model Higgs boson is expected to be produced via the Bjorken mechanism where the Z^0 boson is produced in association with the Higgs boson via the process $e^+e^- \rightarrow H^0Z^0$. If the Z^0 boson is produced on shell it leaves no phase space for a Higgs boson with a mass above $\sqrt{s} - m_{Z^0}$ to be produced. This sets up a natural wall for the maximum Higgs mass one can probe at LEP 200. This wall is 97.8, 106.8 and 108.8 GeV/c^2 for $\sqrt{s}$= 189,198 and 200 GeV respectively. In principle there are two ways this wall could be penetrated. The Z^0 boson could be produced off shell in the Bjorken process, or, in the case of electrons or neutrinos in the final state, the Higgs could be produced via the W^+W^- and Z^0Z^0 fusion processes. However, the cross sections for the fusion processes, even though they exceed that of the Bjorken processes for a Higgs mass above the wall, are too small to produce a detectable signal with luminosities less than 200 pb^{-1} (Fig. 2).

The Higgs boson decays predominantly to $b\bar{b}(\sim 86\%)$ while the Z^0 decays $\sim 70\%$ to quarks ($q\bar{q}$), $\sim 20\%$ to neutrinos ($\nu\bar{\nu}$), and $\sim 9\%$ to charged leptons (l^+l^-).

In this analysis we have addressed the principal final state topologies, which account for about 84% of all SM Higgs boson final states, namely:
(i) the four jet channel, $e^+e^- \rightarrow Z^0H^0 \rightarrow q\bar{q}b\bar{b}(\sim 60\%)$;
(ii) the missing energy channel, mainly from $e^+e^- \rightarrow Z^0H^0 \rightarrow \nu\bar{\nu}b\bar{b}$, with a small contribution from the W^+W^- fusion process $e^+e^- \rightarrow \nu\bar{\nu}H^0(\sim 18\%)$;
(iii) the muon and electron channels, predominantly from $e^+e^- \rightarrow Z^0H^0 \rightarrow \mu^+\mu^- q\bar{q}$ and $e^+e^- q\bar{q}$, with the latter including a small contribution from the Z^0Z^0 fusion process $e^+e^- \rightarrow e^+e^- H^0(\sim 6\%)$.

The cuts described in the rest of Section 3 were tuned so as to reproduce the efficiencies and expected backgrounds to the level of 10% at $\sqrt{s}$=183 GeV[10], and then applied at the higher centre-of-mass energies.

3.1 Missing Energy Channel

The $e^+e^- \rightarrow \nu\bar{\nu}H^0 \rightarrow \nu\bar{\nu}b\bar{b}$ process amounts to approximately 18% of the Higgs boson production cross section with a small contribution from the W^+W^- fusion process $e^+e^- \rightarrow \nu\bar{\nu}H^0 \rightarrow \nu\bar{\nu}b\bar{b}$. These events are characterized by large missing momentum and two energetic, acoplanar, hadronic jets containing b-flavoured hadrons. The dominant backgrounds are mismeasured $Z^0/\gamma^* \rightarrow q\bar{q}$ events, four-fermion processes with neutrinos in the final state, such as $Z^0Z^{0(*)} \rightarrow \nu\bar{\nu}q\bar{q}$, $W^+W^- \rightarrow \ell^{\pm}\nu q\bar{q}$, $W^{\pm}e^{\mp}\nu \rightarrow q\bar{q}\ e^{\mp}\nu$ with the charged lepton escaping detection and, in general, events in which particles go undetected down the beam pipe such as $e^+e^- \rightarrow Z^0\gamma$ and two-photon events. For most of these backgrounds, the missing momentum vector points close to the beam direction, while signal events tend to have missing momentum in the transverse plane. However, though most of the above mentioned four-fermion background can be largely reduced via b-tagging, the $Z^0Z^{0(*)} \rightarrow \nu\bar{\nu}b\bar{b}$ process is an irreducible background.

The event selection proceeds as follows:

(1) To reduce two-photon and beam-wall interactions, the number of tracks should be greater than six. The fraction of energy deposited in the region $|\cos\theta| > 0.90$ must not exceed 50% of the total visible energy in the event. In addition, a large fraction of the hadronic background is removed by requiring that the fraction of visible energy of the event be less than 80% of the centre-of-mass energy, $E_{\rm vis}/\sqrt{s} < 0.80$.

(2) To remove backgrounds in which particles go undetected down the beam pipe, the polar angle, $\theta_{\rm miss}$, of the missing momentum ($\vec{P}_{\rm miss} = -\vec{P}_{\rm vis}$) must satisfy $|\cos\theta_{\rm miss}| < 0.9$. The z-component of the visible momentum, $P^z_{\rm vis}$, is required to be less than 35 GeV/c.

(3) The remaining two-photon background is reduced further by requiring that the transverse momentum of the event with respect to the beam direction, $P^T_{\rm vis} > 8$ GeV/c.

(4) The remaining events are reconstructed as two-jet events using the Durham algorithm. The axes of both jets are required to have a polar angle satisfying $|\cos\theta_{\rm jet}| < 0.9$, to ensure good containment.

(5) The remaining background from $\rm Z^0/\gamma^* \to q\bar{q}$ is characterized by two jets that tend to be back-to-back with small acoplanarity angles (the acoplanarity angle is defined as $180^\circ - \phi_{jj}$ where ϕ_{jj} is the angle between the two jets in the plane perpendicular to the beam axis), in contrast to signal events in which the jets are expected to have some acoplanarity angle due to the boost of the Higgs boson. This background is suppressed by requiring that the jet-jet acoplanarity angle be larger than 5°.

(6) Since the Higgs boson recoils against a $\rm Z^0$ boson decaying into a pair of neutrinos, the signal would have a missing mass close to $m_{\rm Z^0}$. The remaining backgrounds, predominantly from well contained multi-hadron and four-fermion events including semi-leptonic $\rm W^+W^-$ decays, typically have small missing masses. These backgrounds are reduced by the missing mass requirement $(60\ {\rm GeV/c^2})^2 < m^2_{\rm miss} < (120\ {\rm GeV/c^2})^2$.

(7) $\rm W^+W^-$ events with one of the W bosons decaying leptonically and the other decaying into hadronic jets are rejected by requiring that the events have no isolated leptons.

In this context, leptons are low-multiplicity jets with one (two or three) tracks and possibly associated electromagnetic or hadronic energy clusters, confined to a cone of 6° half-angle, having an invariant mass less than 2.5 GeV/$\rm c^2$ and momentum in excess of 5 GeV/c. The lepton is considered isolated if the fraction of energy in this cone is larger than 88% of the energy contained in an isolation cone of 25° half-angle. The energies are calculated from the tracks and calorimetric clusters in the two cones. The isolation cone is not allowed to contain another track.

(7) Finally, both jets are tagged as b-jets using the fast simulation b-tagger with the efficiency parameter set to 72%.

The detection efficiencies and the expected backgrounds for $\sqrt{s}$ = 189 and 200 GeV are given in Tables 1 and 2. An example of the expected signal on top of the expected background is given in Fig. 3 for m_{H^0}=100 GeV/c^2 at $\sqrt{s}$ =198 GeV.

m_{H^0} (GeV/c^2)	85	90	95	100	105	110
$\sqrt{s}$ =189	35	33	31	24	21	16
$\sqrt{s}$ =198	33	33	33	33	30	28

Table 1: *The efficiencies (in %) for Higgs detection for the missing energy channel.*

Background Source	Hadronic	4-fermions ($\mathrm{Z}^0\mathrm{Z}^0$ and W^+W^-)
$\sqrt{s}$ =189	15	60
$\sqrt{s}$ =198	10	70

Table 2: *The expected background (for the combined LEP) (in fb) for the missing energy channel,* $e^+e^-\rightarrow \mathrm{H}^0\mathrm{Z}^0\rightarrow b\bar{b}\nu\bar{\nu}$.

3.2 The Four Jet Channel

The process $\mathrm{e^+e^-}\rightarrow \mathrm{Z^0H^0}\rightarrow \mathrm{q\bar{q}b\bar{b}}$ amounts to approximately 60% of the SM Higgs boson production cross section. It is characterized by four energetic hadronic jets, large visible energy and the presence of b-flavoured hadron decays. The backgrounds are $\mathrm{Z}^0/\gamma^*\rightarrow \mathrm{q\bar{q}}$ with and without initial state radiation accompanied by hard gluon emission as well as four-fermion processes, in particular $\mathrm{e^+e^-}\rightarrow W^+W^-$,$\mathrm{Z^0Z^0}$. The suppression of these backgrounds relies on the kinematic reconstruction of the Z^0 boson and on the identification of b quarks from the Higgs boson decay.

The following cuts are applied:

(1) The events must be balanced to qualify as having a hadronic final state.

(2) The radiative process $\mathrm{e^+e^-}\rightarrow \mathrm{Z^0}\gamma\rightarrow \mathrm{q\bar{q}}\gamma$ is largely reduced by requiring that the effective centre-of-mass energy, $\sqrt{s'}$, obtained by discarding a reconstructed radiative photon from the event, is at least 160 GeV.

(3) The final state particles are grouped into four jets using the Durham algorithm. The jet resolution parameter, y_{34}, at which the number of jets changes from 3 to 4, is required to be larger than 0.005.

(4) The angle between any pair of jets should be bigger than 40^o.

(5) The spherical nature of the Higgs events is taken into account by requiring that the sphericity of the events, S, be bigger than 0.1.

(6) Each of the four jets are required to contain at least two charged tracks.

(7) The $e^+e^- \to H^0Z^0$ hypothesis is tested by a kinematic fit which, in addition to the energy and momentum conservation constraints, also forces two of the four jets which recoils against a b-tagged pair (where both jets are tagged as b-jets with the efficiency parameter set to 72%) to have an invariant mass equal to the Z^0 boson mass (5C-fit). This fit is applied in turn to all six possible associations of the four jets to the Z^0 and H^0 bosons. The fit is required to converge for at least one combination and the combination with the highest χ^2 probability is chosen to identify the Higgs and the Z^0 di-jets.

The detection efficiencies and the expected backgrounds for $\sqrt{s}$ = 189 and 200 GeV are given in Tables 3 and 4. An example of the expected signal on top of the expected background is given in Fig. 4 for m_{H^0}=100 GeV/c^2 at $\sqrt{s}$ =198 GeV. One can note the large tail of the signal shape due to the association of incorrect di-jets to the Higgs boson.

m_{H^0} (GeV/c^2)	85	90	95	100	105	110
$\sqrt{s}$ =189	41	40	37	30	27	21
$\sqrt{s}$ =198	42	42	37	37	36	33

Table 3: *The efficiencies (in %) for Higgs detection for the four-jets channel,* $e^+e^- \to H^0Z^0 \to b\bar{b}q\bar{q}$.

Background Source	Hadronic	4-fermions (Z^0Z^0 and W^+W^-)
$\sqrt{s}$ =189	98	235
$\sqrt{s}$ =198	96	270

Table 4: *The expected background (for the combined LEP) (in fb) for the four-jets channel.*

3.3 The Electron and Muon Channels

The $\ell^+\ell^-q\bar{q}$ (ℓ = e or μ) final states arise mainly from the process $e^+e^- \to Z^0H^0 \to \ell^+\ell^-q\bar{q}$. They amount to approximately 6% of the Higgs boson production cross section with a small contribution from the Z^0Z^0 fusion process $e^+e^- \to e^+e^-H^0 \to e^+e^-q\bar{q}$.

The analysis adopted concentrates on those final states proceeding through the first process. These yield a clean experimental signature in the form of large visible energy, two energetic, isolated, oppositely-charged leptons of the same species reconstructing to the Z^0 boson mass, and

two energetic hadronic jets carrying signs of b-flavoured hadrons. The dominant backgrounds are four-fermion processes (Z^0Z^0).

The selection proceeds as follows:

(1) The selected events are required to have at least six tracks and must satisfy the relation $E_{\rm vis} > 0.6\sqrt{s}$.

(2) The selected events must contain at least one pair of oppositely charged, same flavour leptons (e or μ).

If more than one pair of leptons of the same flavour is found, the pair with invariant mass closest to the Z^0 boson mass is selected.

(3) Both leptons in the candidate pair must have an energy larger than 20 GeV with at least one of them larger than 30 GeV.

(4) The rest of the event, obtained by excluding the candidate lepton pair, is reconstructed as two jets using the Durham algorithm. An explicit lepton isolation cut is made to reject the remaining background from $Z^0/\gamma^* \to q\bar{q}(\gamma)$ with leptons close to the hadronic jets, by requiring that each of the leptons has a transverse momentum, calculated with respect to the nearest jet axis, larger than 10 GeV/c.

(5) The selected events must have a lepton pair with an invariant mass consistent with the Z^0 boson mass, i.e. the invariant mass of the lepton pair must lie between 70 GeV/c^2 and 100 GeV/c^2.

(6) Finally one of the two jets is required to carry b-flavour. At $\sqrt{s}$ =189 GeV the b-tag efficiency parameter is tighter (efficiency=60%) than at 198 GeV (efficiency=70%) because of the reduced background in the vicinity of the Higgs at the higher centre-of-mass energy.

The detection efficiencies and the expected backgrounds for $\sqrt{s}$ = 189 and 200 GeV are given in Tables 5 and 6. An example of the expected signal on top of the expected background is given in Fig. 5 for m_{H^0}=100 GeV/c^2 at $\sqrt{s}$ =198 GeV. One can see the excellent mass resolution of the charged leptonic channel.

m_{H^0} (GeV/c^2)	85	90	95	100	105	110
$\sqrt{s}$ =189	60	60	60	51	37	26
$\sqrt{s}$ =198	66	66	66	66	66	53

Table 5: *The efficiencies (in %) for Higgs detection for the charged-leptonic channel,* $\ell^+\ell^-q\bar{q}$ *(*ℓ *= e or* μ*).*

Background Source	4-fermions (Z^0Z^0)
$\sqrt{s}$ =189	43
$\sqrt{s}$ =198	81

Table 6: *The expected background (for the combined LEP) (in fb) for the charged-leptonic channel.*

4 The Statistical Procedures

The statistical procedure used here [7] to analyze the output of the fast Monte Carlo simulation has been used by DELPHI in its Standard Model Higgs boson search [8] and is one of four procedures used recently by the LEP Working Group for Higgs boson searches to combine the Higgs search results of the four LEP experiments [2]. Since this procedure is rather different from the one used in the workshop, it will be described in some detail here, after a short review of the terminology used to describe search results (from the viewpoint of classical or frequentist statistics).

4.1 Confidence levels

In order to quantify the results of a search, a test-statistic X must be defined which discriminates signal [4] from background experimental results. The test-statistic may be as simple as the total number of selected events, or it may be a complex function of both the number of selected events in distinct search channels and one or more properties of the selected events (such as the invariant mass of the Higgs candidate used in this analysis). The probability distribution of the test-statistic may be known exactly (e.g. Poisson statistics for single-channel counting experiments) or it may be derived by Monte Carlo or other integration techniques for more complex search results.

The confidence in the signal plus background hypothesis CL_{s+b} is defined as the probability to obtain $X < X_{obs}$ in gedanken signal experiments for a specified signal hypothesis, where X_{obs} is the value of the test-statistic observed for the experiment. The confidence in the background hypothesis CL_b is defined as the probability to observe $X < X_{obs}$ in gedanken background experiments. When performing a search with small expected signal rates and non-negligible background rates, the probability of excluding the signal more strongly than if the expected background rate were 0 may be substantial (in such experiments the most probable signal rate may be unphysical). Background fluctuations may also result in such a strong signal exclusion that even infinite Higgs mass (0 signal rate) may be excluded at or above the 95% CL. To prevent apriori such unaesthetic, but nevertheless formally valid, results from occurring, we

[4] A "signal experiment" in the rest of this report implicitly includes the expected background contribution.

consider the ratio $CL_s = CL_{s+b}/CL_b$ suggested in [9] as a conservative approximation to the signal confidence one might have obtained in the absence of background.

4.2 The likelihood ratio test-statistic

The probability density ratio or likelihood ratio (as it is called when used in a Bayesian context) is used here in the statistical procedure as the test-statistic. Although not always practical, the likelihood ratio makes the most efficient use of the information available in a search result in a manner similar to the way the principle of maximum likelihood gives the most efficient estimators of parameters in a measurement. For this work we have included the number of selected events and the measured masses of the Higgs candidates in the likelihood ratio $Q(m_{\mathrm{H}^0})$:

$$Q(m_{\mathrm{H}^0}) = \frac{\prod_{i=1}^{N_{chan}} \frac{e^{-(s_i(m_{\mathrm{H}^0})+b_i)}(s_i(m_{\mathrm{H}^0})+b_i)^{n_i}}{n_i!}}{\prod_{i=1}^{N_{nchan}} \frac{e^{-b_i} b_i^{n_i}}{n_i!}} \frac{\prod_{j=1}^{n_i} \frac{s_i(m_{\mathrm{H}^0}) S_i(m_{ij}, m_{\mathrm{H}^0}) + b_i B_i(m_{ij})}{s_i(m_{\mathrm{H}^0})+b_i}}{\prod_{j=1}^{n_i} B_i(m_{ij})}, \qquad (1)$$

where n_i is the number of events selected in each channel i, m_{ij} is the mass of the Higgs boson candidate measured for each of the events j, $s_i(m_{\mathrm{H}^0})$ and b_i are the integrated signal and background rates, and $S_i(m, m_{\mathrm{H}^0})$ and $B_i(m)$ are the probability distribution functions of the mass of the Higgs boson candidates for the signal (no background) and background respectively. It is to be noted that since all the signal and background expectations depend on the centre-of-mass energy, each energy point considered in a given combination contributed three independent search channels to the likelihood ratio.

The probability distributions of the likelihood ratio for signal and background experiments are obtained by Monte Carlo generation of experiments according to the relevant hypotheses. The observed confidence levels, the discovery and exclusion potentials defined in the next section, and, if necessary, the expected confidences, are all derived from these probability distributions.

4.3 Exclusion and discovery potentials

The exclusion potential is defined as the probability to exclude a signal hypothesis if it is false, in other words, the fraction of gedanken background experiments which satisfy $1 - CL_s \geq 95\%$. The discovery potential is defined as the probability to confirm the signal hypothesis if it is true and exclude the background hypothesis with a significance of 5σ, in other words, the fraction of signal gedanken experiments with $1 - CL_b \leq 5.7 \times 10^{-7}$.

The exclusion potential for a hypothetical experiment is illustrated in Fig. 6, where the probability distributions and their integrals, the confidences, are shown. The shaded areas correspond to the confidences observed for an imaginary experiment with $2\ln(Q_{obs}) = 3$; the signal hypothesis for this experiment is excluded at the 95% CL. In addition, the shaded area of the background distribution is the exclusion potential of the experiment - this can be read off from the integrals in the lower plot, as indicated by the crossed lines.

The discovery potential for another hypothetical experiment is illustrated in Fig. 7 where the probability distributions of $2\ln(Q)$ for signal and background experiments are shown in addition to the cumulative distributions (the confidences). The shaded area in the upper plot represents the signal gedanken experiments which have a background confidence in the discovery region, i.e. $1 - CL_b \leq 5.7 \times 10^{-7}$.

4.4 Exclusion and discovery limits

The exclusion limit of the Higgs boson mass is the value of m_{H^0} at which 50% of background experiments are expected to lead to a 95% or better CL exclusion of the signal hypothesis. In a similar manner, the discovery limit of the Higgs boson mass is the value of m_{H^0} for which 50% of signal experiments are expected to have a significance of 5σ or better ($1-CL_b \leq 5.7\times10^{-7}$). These definitions are the same as those used in the LEP200 workshop.

From Fig. 7 it should be clear that there is no guarantee of 5σ discovery even if the true mass is at or below the discovery limit and that it is possible to make a 5σ discovery even if the true mass is somewhat above the discovery limit.

Fig. 8 shows how the exclusion potential (a) and the discovery potential (b) depend on m_{H^0} for a given experimental configuration (30 pb^{-1} of integrated luminosity per experiment at $\sqrt{s}$ = 189 GeV). The exclusion limit of 94.4 $\mathrm{GeV/c^2}$ (vertical line in (a)) is where the expected exclusion confidence crosses the horizontal line at 95% . The discovery limit of 86.9 $\mathrm{GeV/c^2}$ (vertical line in (b)) is where the "5σ" discovery curve crosses the horizontal line at 50%.

5 Results

Using the statistical procedures described in Section 4, the simulation results (efficiencies, background and signal expectations) are interpreted in terms of exclusion and discovery sensitivities for the Standard Model Higgs boson. In the case of exclusion we also examine an interpretation in terms of the MSSM (Minimal Supersymmetric Standard Model).

In the MSSM neutral Higgs bosons may be produced by the process $\mathrm{e^+e^-}\rightarrow\mathrm{Z^0h^0}$, or $\mathrm{e^+e^-}\rightarrow\mathrm{A^0h^0}$. In this case the lightest CP-even Higgs boson $\mathrm{h^0}$ plays a role analogous to $\mathrm{H^0}$ in the Standard Model. In this paper we limit ourself to the SM-like production process. The cross-section for this process can be written as

$$\sigma_{\mathrm{Zh}} = \sin^2(\beta-\alpha)\ \sigma^{\mathrm{SM}}_{\mathrm{ZH}} \tag{2}$$

where $\sigma^{\mathrm{SM}}_{\mathrm{ZH}}$ is the cross-section for the SM process $\mathrm{e^+e^-}\rightarrow\mathrm{Z^0H^0}$. The angle β is defined in terms of the ratio of the vacuum expectation values of the two scalar fields, $\tan\beta = v_2/v_1$, and α is the mixing angle of the CP-even ($\mathrm{h^0}$,$\mathrm{H^0}$) fields.

In the context of this paper we estimate the exclusion sensitivity for a Supersymmetric light Higgs boson by measuring how much the SM Higgs cross section can be scaled down and still result in an exclusion (on the average) at the 95% C.L. This is interpreted in terms of upper limits on $\sin^2(\beta - \alpha)$.

5.1 Excluding the SM Higgs Boson

Fig. 9 shows the luminosity needed to exclude the signal hypothesis in 50% of background experiments at the 95% or greater C.L. It is shown as a function of the Higgs boson mass for various combinations of centre-of-mass energies. The curves (from left to right) shows the exclusion sensitivity for $\sqrt{s}$=189 and 198 GeV. Shown next is the sensitivity if one combines the prospective sensitivity of 150 pb^{-1} collected at $\sqrt{s}$=189 GeV with the prospective sensitivity at $\sqrt{s}$=198 and 200 GeV. The star on the right side indicates the exclusion sensitivity if one stops collecting data after 100 pb^{-1} at $\sqrt{s}$=198 GeV and upgrades to $\sqrt{s}$=200 GeV where additional 50 pb^{-1} are collected. One can see from the plot that from the SM Higgs point of view there is not much to gain by increasing the luminosity above 50 pb^{-1} at $\sqrt{s}$=189 GeV and that the combination of lower centre-of-mass energy data with higher centre-of-mass data does not improve the sensitivity for a luminosity above 50 pb^{-1}. It is also seen that the exclusion sensitivity when collecting 200 pb^{-1} at $\sqrt{s}$=198 GeV (m_{H^0}=107.0 GeV/c^2) is comparable to that obtained if one trades the last 100 pb^{-1} collected at $\sqrt{s}$=198 GeV with 50 pb^{-1} collected at $\sqrt{s}$=200 GeV (m_{H^0}=107.6 GeV/c^2). However from Table 7 where some specific points are given it is clear that if one can provides higher luminosity at $\sqrt{s}$=200 GeV (*i.e.* if the trade in is better than 50%), the search sensitivity is improved. For example, if the additional luminosity collected at $\sqrt{s}$=200 GeV is 100pb^{-1} rather than 50 pb^{-1}, the exclusion sensitivity improves significantly from m_{H^0}=107.6 to 108.5 GeV/c^2 which brings the search sensitivity almost to its kinematical limit (m_{H^0}=108.8 GeV/c^2). It is interesting to note that if the 200 pb^{-1} were collected at $\sqrt{s}$=200 rather than $\sqrt{s}$=198 GeV the kinematical wall would be penetrated and the exclusion sensitivity would be saturatied at m_{H^0}= 109.1 GeV/c^2.

5.2 Setting upper Limits on $\sin^2(\beta - \alpha)$

Prospective upper limits on $\sin^2(\beta - \alpha)$ as a function of the light MSSM Higgs mass are shown in Fig. 10. Two sets of curves are shown. The first set examines the effect of adding 150 pb^{-1} collected at $\sqrt{s}$=189 GeV to 100 pb^{-1} collected at the higher centre-of-mass energy of 198 GeV. The second set examines the trade in of 100 pb^{-1} and 50 pb^{-1} collected at $\sqrt{s}$=198 and 200 GeV respectively in return to 200 pb^{-1} collected at $\sqrt{s}$=198 GeV.

In the first case it is clearly seen that from the MSSM Higgs point of view one wins by adding lower centre-of-mass data to higher centre-of-mass data (in contrast to the SM Higgs case). The same trend is seen also in the second set, though by upgrading the centre-of-mass to a higher energy (even increasing it by only 2 GeV) one wins at the high Higgs mass region (where $\sin^2(\beta - \alpha)$ is close to 1.0, and one probes the SM Higgs exclusion region). Again this

gain will increase if more luminosity could be provided at the higher centre-of-mass energy.

5.3 Discovering the SM Higgs Boson

Figure 11 shows the luminosity needed to discover in 50% of signal+background experiments at the 5σ level a SM Higgs boson as a function of the Higgs boson mass for various combinations of CM energies. The curves (from left to right) show the discovery sensitivity for $\sqrt{s}$=189 and 198 GeV. Next shown is the sensitivity if one combines the prospective sensitivity of 150 pb^{-1} collected at $\sqrt{s}$=189 GeV with the prospective sensitivity at $\sqrt{s}$=198 and 200 GeV. The star on the right side indicates the discovery sensitivity if one stops collecting data after 100 pb^{-1} at $\sqrt{s}$=198 GeV and upgrades to $\sqrt{s}$=200 GeV where additional 50 pb^{-1} are collected. One can see from the plot that the discovery sensitivity for the SM Higgs boson saturates at $\sqrt{s}$=189 GeV with an integrated luminosity of 100 pb^{-1}. It is also seen that the average discovery sensitivity when collecting 200 pb^{-1} at $\sqrt{s}$=198 GeV (m_{H^0}=104.5 GeV/c^2) is comparable to that obtained if one trades the last 100 pb^{-1} collected at $\sqrt{s}$=198 GeV with 50 pb^{-1} collected at $\sqrt{s}$=200 GeV (m_{H^0}=104.2 GeV/c^2). However from Table 7 where some specific points are given it is clear that if one can provides higher luminosity at $\sqrt{s}$=200 GeV (*i.e.* if the trade in is better than 50%), the discovery sensitivity is improved and the search benefits. For example, if the additional luminosity collected at $\sqrt{s}$=200 GeV is 100 pb^{-1} rather than 50 pb^{-1}, the discovery sensitivity improves by more than 1.5 GeV/c^2 from m_{H^0}=104.2 to 105.8 GeV/c^2. It is to be noted that collecting 200 pb^{-1} at $\sqrt{s}$=200 GeV can discover a Higgs up to m_{H^0}= 106.9 GeV/c (to be comparable with a discovery sensitivity of m_{H^0}= 104.5 GeV/c if the 200 pb^{-1} are collected at the lower centre-of-mass energy of 198 GeV).

Some specific points are given in Table 7.

$\mathcal{L}$ @189 (pb^{-1})	$\mathcal{L}$ @198 (pb^{-1})	$\mathcal{L}$ @200 (pb^{-1})	Exclusion (GeV/c^2)	Discovery (GeV/c^2)
0	200	0	107.0	104.5
100	150	50	107.9	105.1
150	150	50	108.0	105.1
150	200	0	107.0	104.5
150	0	100	108.0	103.3
150	0	150	108.7	106.0
150	0	200	109.1	106.9
150	100	50	107.6	104.2
100	200	0	107.0	104.5
100	100	50	107.6	104.2
150	100	100	108.5	105.8

Table 7: *The exclusion and discovery limits for the SM Higgs boson mass for various combinations of integrated luminosities at various centre-of-mass energies.*

5.4 Discovering a Higgs boson with $m_{\mathrm{H}^0} \sim m_{\mathrm{Z}^0}$

In [1] the discovery potential was significantly worsened in the region mH$\sim$mZ for $\sqrt{s}$=205 GeV. This worsening manifested itself as a broad bump in the luminosity discovery potential plot around $m_{\mathrm{H}^0} \sim m_{\mathrm{Z}^0}$. A similar bump is not visible in Fig. 11. In order to trace the reason we have calculated the discovery potential fixing the Higgs production cross section to its value at m_{H^0}=85 GeV/c^2 through the all mass range. The result indicated a clear worsening of the discovery potential around $m_{\mathrm{H}^0} \sim m_{\mathrm{Z}^0}$ with a shape of a broad bump which is due to the effective event selection, the broadness of the mass distributions, and the optimal use of the mass information in the statistical analysis. When convoluting this broad bump with the steeply falling Higgs production cross-section at higher masses the bump disappears as could be seen in Fig. 11.

5.5 Stability of the Results

How sensitive are the results to systematic uncertainties? To answer this question we have degraded the b-tag performance by decreasing the purity by a factor 2. The effect on the exclusion sensitivity was less than 0.5 GeV/c^2 while the effect on the discovery sensitivity was of the order of 1 GeV/c^2.

However, we believe that our fast MC simplified analysis was very conservative (it did not use likelihood techniques which would certainly improve the efficiencies). The tuning of our analysis was based on the preliminary OPAL 183 GeV [10] analysis. We did not take into account that the experiments keep on improving their analyses from one energy upgrade to the other.

None of the above changes any of the conclusions regarding the running requirements, though the final sensitivity numbers might be a bit better.

6 Conclusions

We have shown that with 200 pb^{-1} (per experiment) collected at $\sqrt{s}$=198 GeV the combined LEP Higgs analysis has the sensitivity to exclude (or discover) a Standard Model Higgs boson close to the kinematical wall (exclude a 107.0 GeV/c^2 Higgs boson at the 95% C.L. or discover a 104.5 GeV/c^2 Higgs boson at the 5σ level).

We have also shown that the combination of the lower centre-of-mass energy data ($\sqrt{s}$=189 GeV) with higher centre-of-mass data ($\sqrt{s}$=198 GeV) improves the sensitivity for probing the light MSSM Higgs boson.

We have shown that the Higgs boson search benefits if the centre-of-mass energy is increased

by 2 GeV provided the delivered integrated luminosity does not degrade by more than a factor of 2 in doing so.

Moreover if LEP would provide high luminosity (200 pb^{-1}) at $\sqrt{s}$=200 GeV the kinematical wall could be penetrated and a Higgs boson with m_{H^0}=109.1 GeV/c^2 could be excluded.

Since a Higgs boson with a mass below 130 GeV/c^2 will be difficult to probe with the LHC, every GeV/c^2 of improved sensitivity counts.

We therefore conclude that, Higgs-wise, it is recommended to run LEP at the maximum energy consistent with an efficient integrated luminosity performance.

Acknowledgments
One of the authors (E.G.) would like to thank Rolf Heuer and the organizers of the Rencontres de Physique de la Vallee' d'Aoste held in La Thuile, March 1998, particularly Giorgio Chiarelli for initiating this work. We would like to thank George Mikenberg, Koichi Nagai and Pippa Wells for their useful advice and help in the preparation of this paper.

References

[1] Higgs Physics, Conveners: M. Carena and P. M. Zerwas in Physics at LEP2, edited by G. Altarelli, T. Sjostrand and F. Zwirner , CERN 96-01,Vol 1, 349-462

[2] Lower Bound for the Standard Model Higgs Boson Mass from Combining the Results of the four LEP Experiments, the LEP Working Group for Higgs Boson Searches, ALEPH,DELPHI,L3 and OPAL, 1st April 1998, CERN-EP/98-046.

[3] D. Brandt in the Proceedings of the 8th LEP Performance Workshop, Chamonix, January 1998, CERN-SL-98-006 DI. See also LEP 2000 Status Report, LEP 2000 Working Group, Editor: G. Cavallari, CERN SL-98-011 DI.

[4] HZHA generator: P. Janot, in *Physics at LEP2*, edited by G. Altarelli, T. Sjöstrand and F. Zwirner, CERN 96-01, vol. 2 (1996), p. 309. For Higgs production cross-sections see also [5].

[5] E. Gross, B. A. Kniehl, and G. Wolf, Z. Phys. **C63** (1994) 417;
erratum *ibid.* **C66** (1995) 32.

[6] PYTHIA 5.721 and JETSET 7.408 generators: T. Sjöstrand, Comp. Phys. Comm. **82** (1994) 74; T. Sjöstrand, LU TP 95-20.

[7] A. L. Read, DELPHI note 97-158 PHYS 737.

[8] DELPHI Collaboration, P. Abreu et al., Eur. Phys. Journ. **C2** (1998) 1.

[9] Particle Data Group: R. M. Barnett et al., *Review of Particle Physics*, Phys. Rev. **D54** (1996) 1.

[10] OPAL Physics Note, PN340,March 1998.

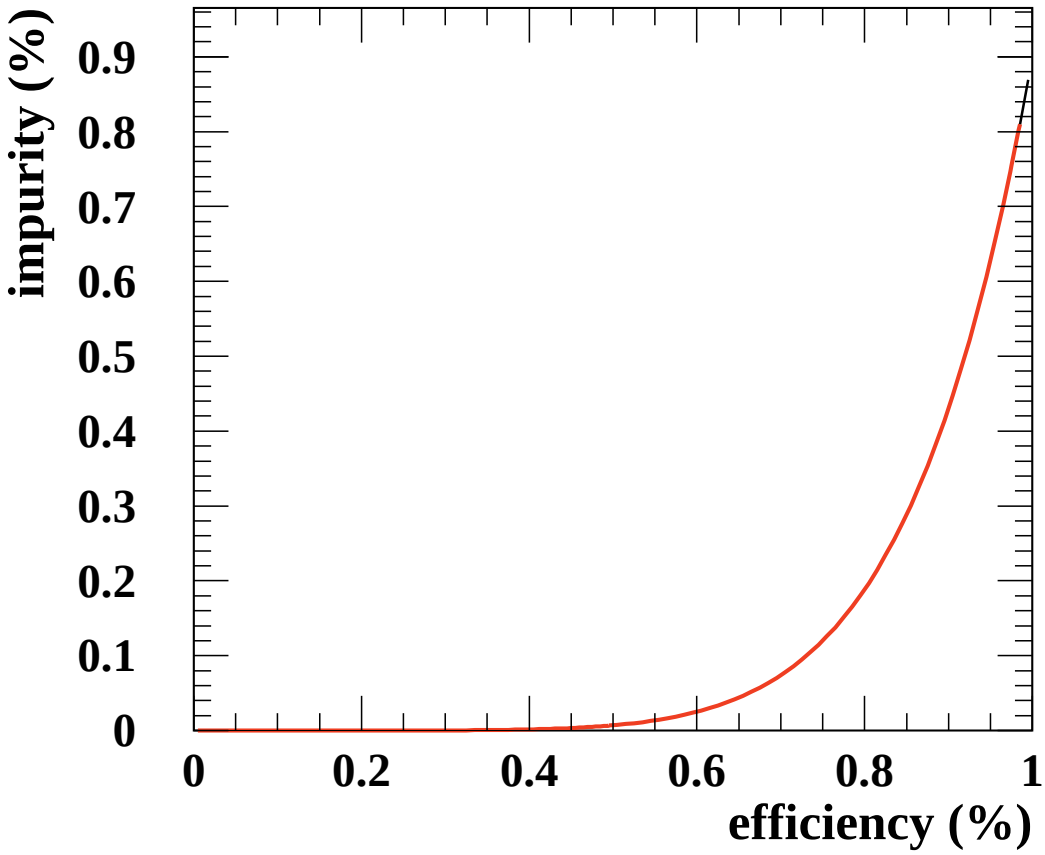

Figure 1: The fast b-tag simulation: impurity versus efficiency.

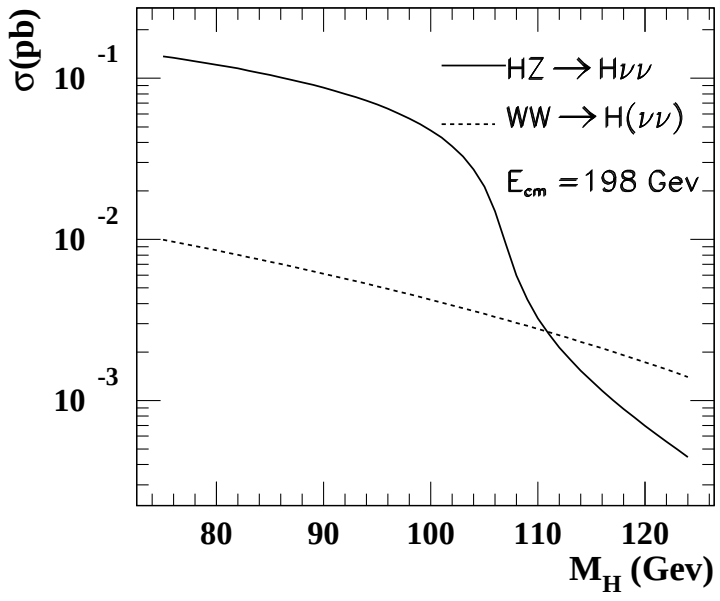

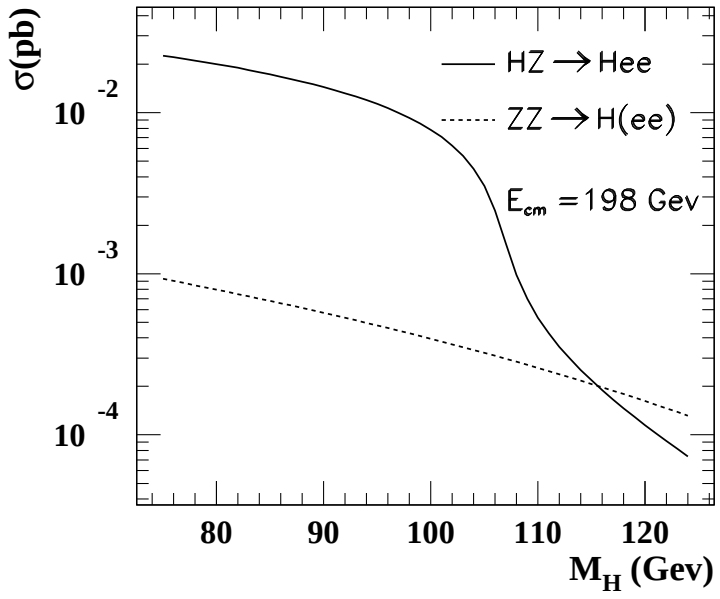

Figure 2: The higgs production cross section in the Bjorken and fusion processes for the missing energy and electronic channels at $\sqrt{s}$ =198 GeV.

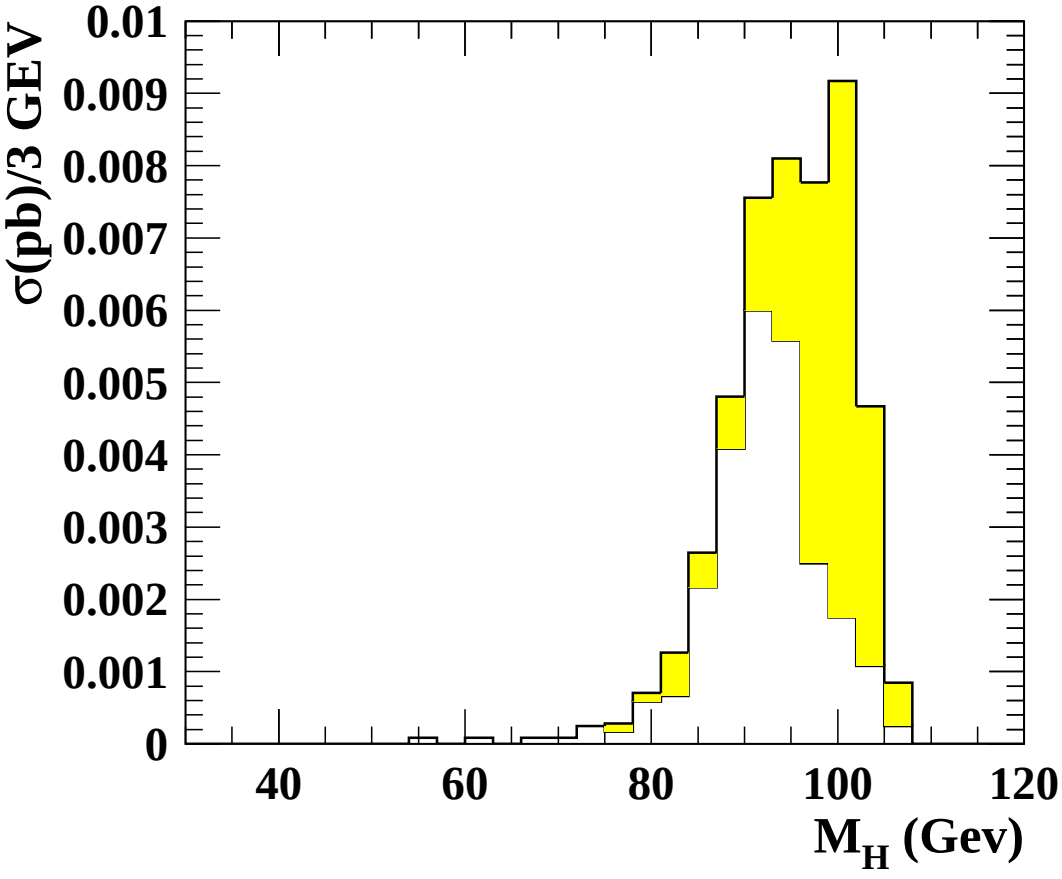

Figure 3: The expected signal on top of the expected background in the missing energy channel for m_{H^0}=100 GeV/c^2 at $\sqrt{s}$ =198 GeV.

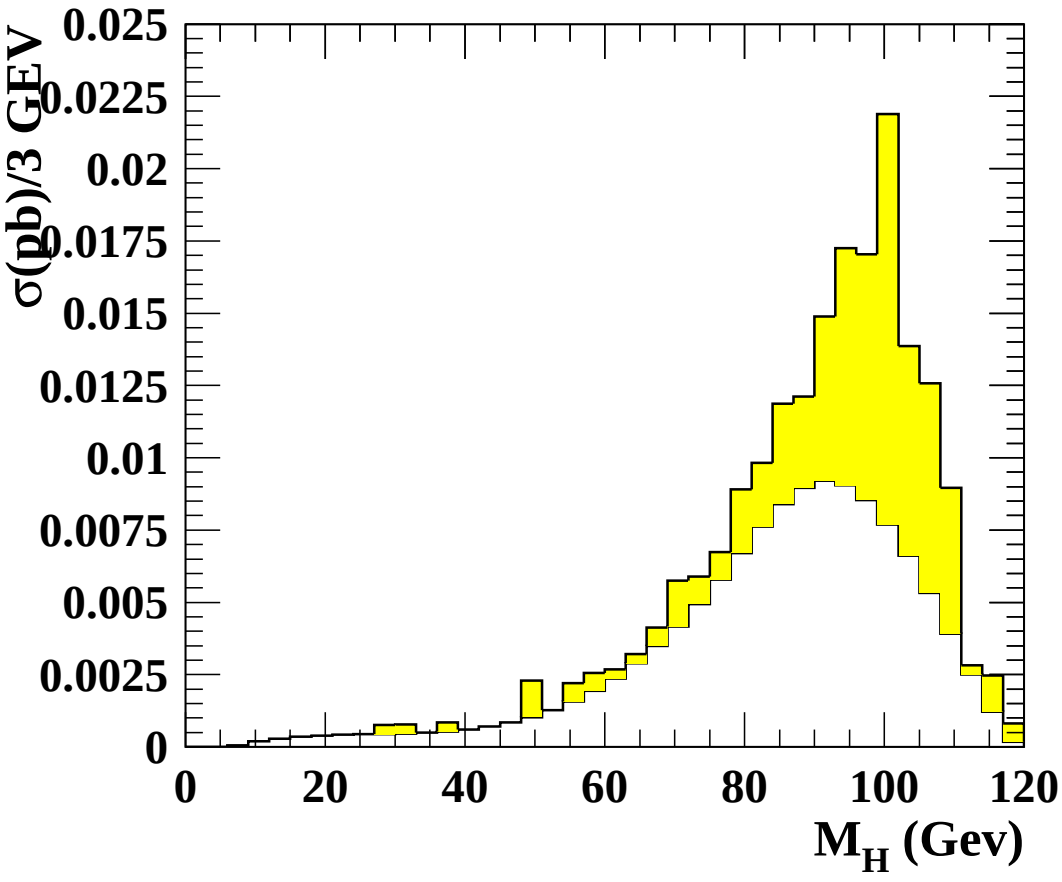

Figure 4: The expected signal on top of the expected background in the 4-jets channel for m_{H^0}=100 GeV/c^2 at $\sqrt{s}$ =198 GeV.

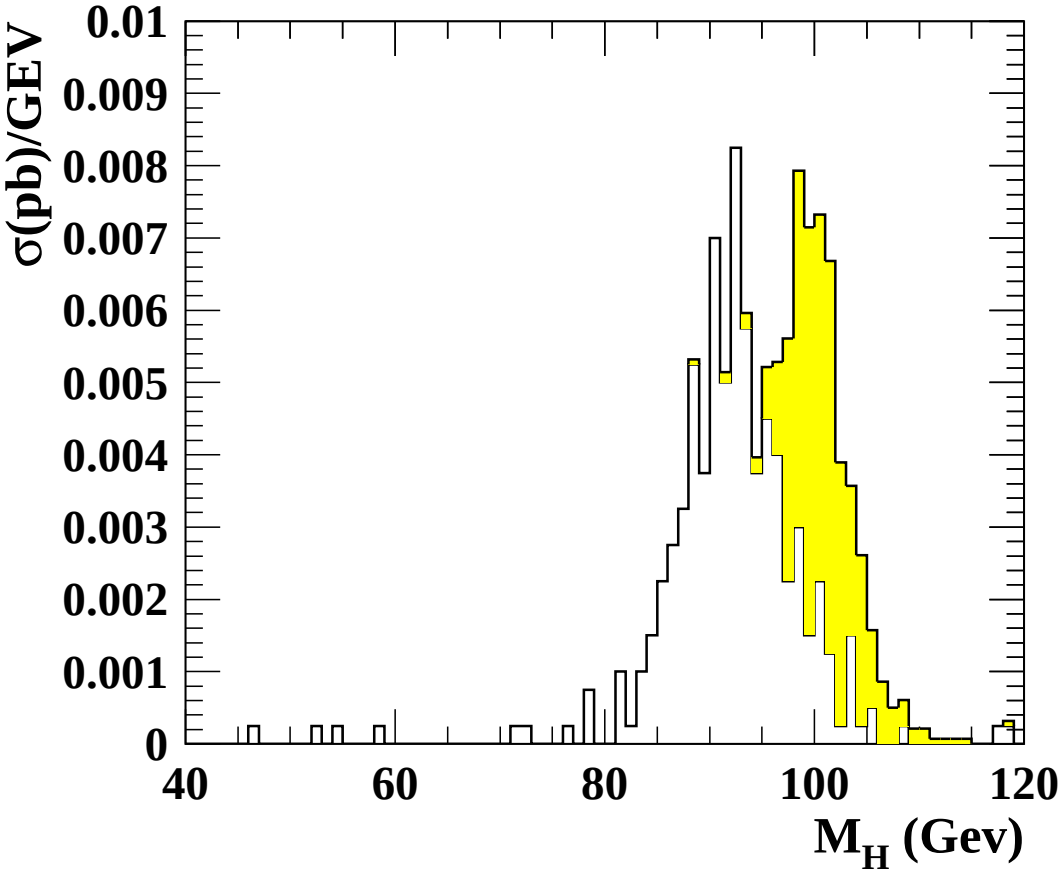

Figure 5: The expected signal on top of the expected background in the electronic-muonic channel for $m_{\mathrm{H^0}}$=100 GeV/c^2 at $\sqrt{s}$ =198 GeV.

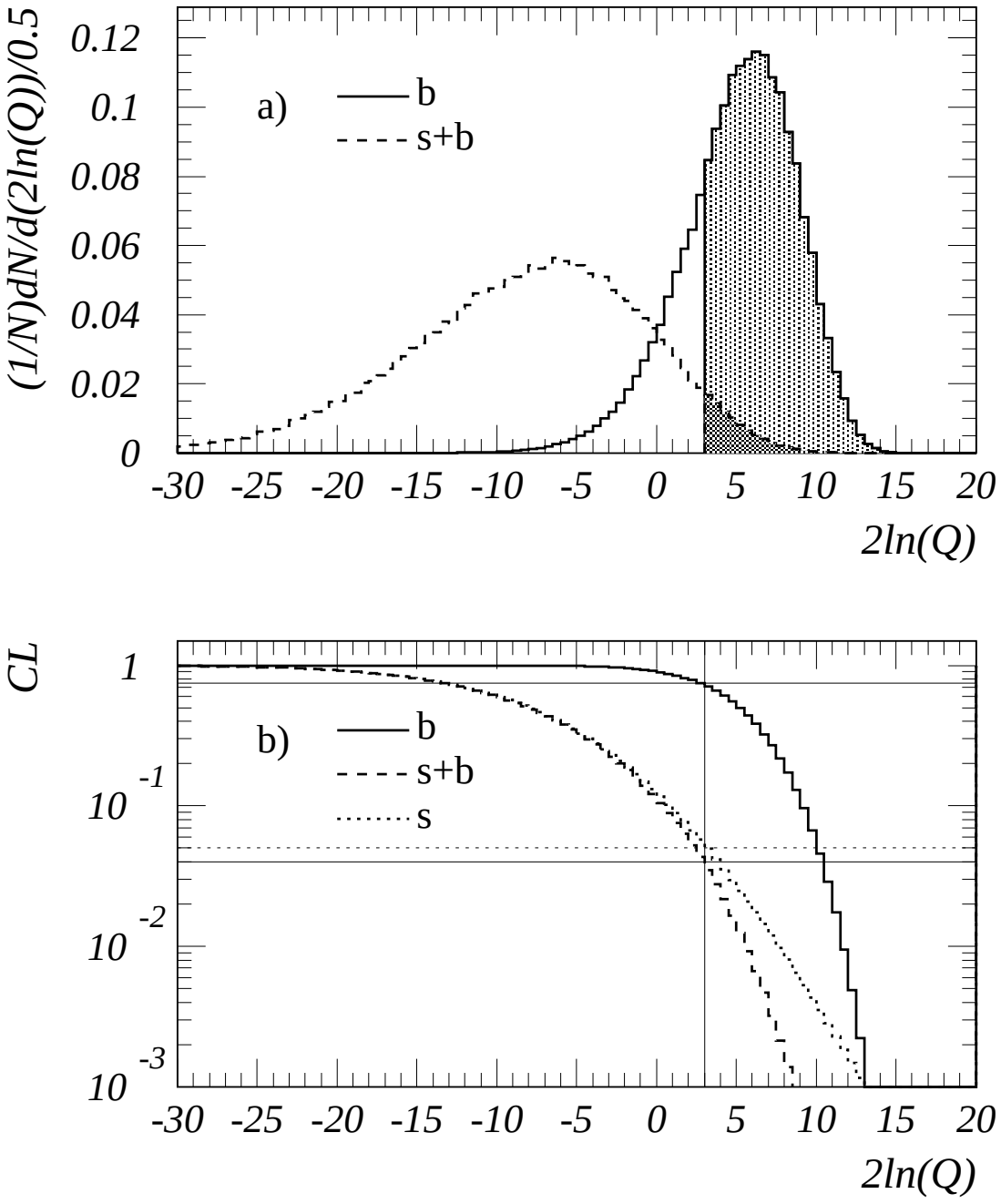

Figure 6: The probability distributions of $2\ln(Q)$ for background "b" and signal "s+b" gedanken experiments (a) and the confidences CL_b, CL_{s+b} and CL_s (b) which are simply the integrals (from right to left) of the distributions in the upper plot. The shaded areas in the upper plot can be read off from the intersection of $2\ln(Q) = 3$ with the confidence curves in the lower plot. The horizontal dotted line at 0.05 shows that the signal hypothesis for this fictitious experiment is excluded at the 95% Confidence Level.

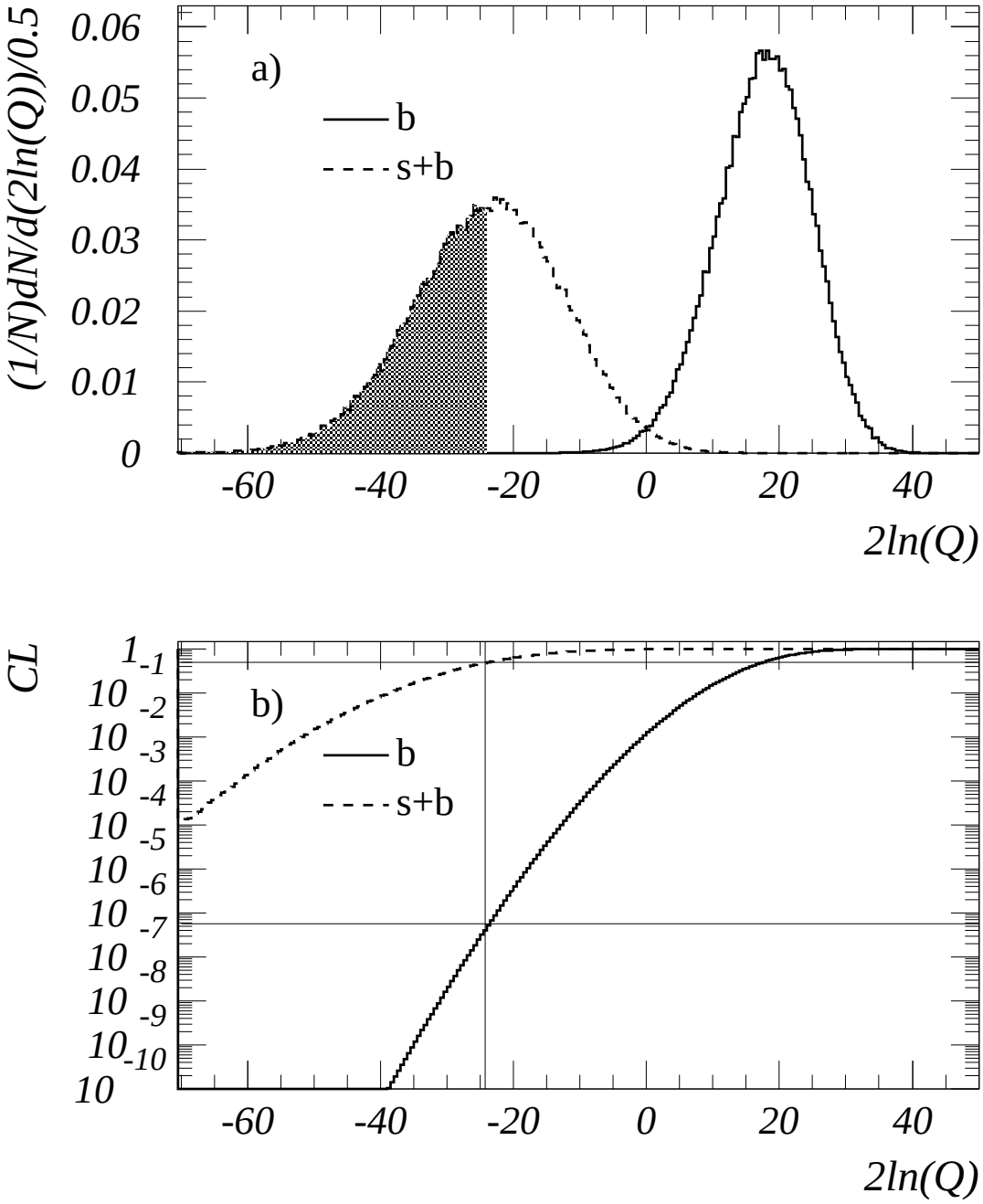

Figure 7: An example of the probability distributions of $2\ln(Q)$ for background "b" and signal "s+b" gedanken experiments (a) and the complements of the confidences $1-CL_b$ and $1-CL_{s+b}$ (b) which are simply the integrals (from left to right) of the distributions in the upper plot. The shaded area in the upper plot (50%) can be read off from the intersection of $1-CL_{s+b}$ with the value of $2\ln(Q)$ for which $1-CL_b = 5.7\times10^{-7}$.

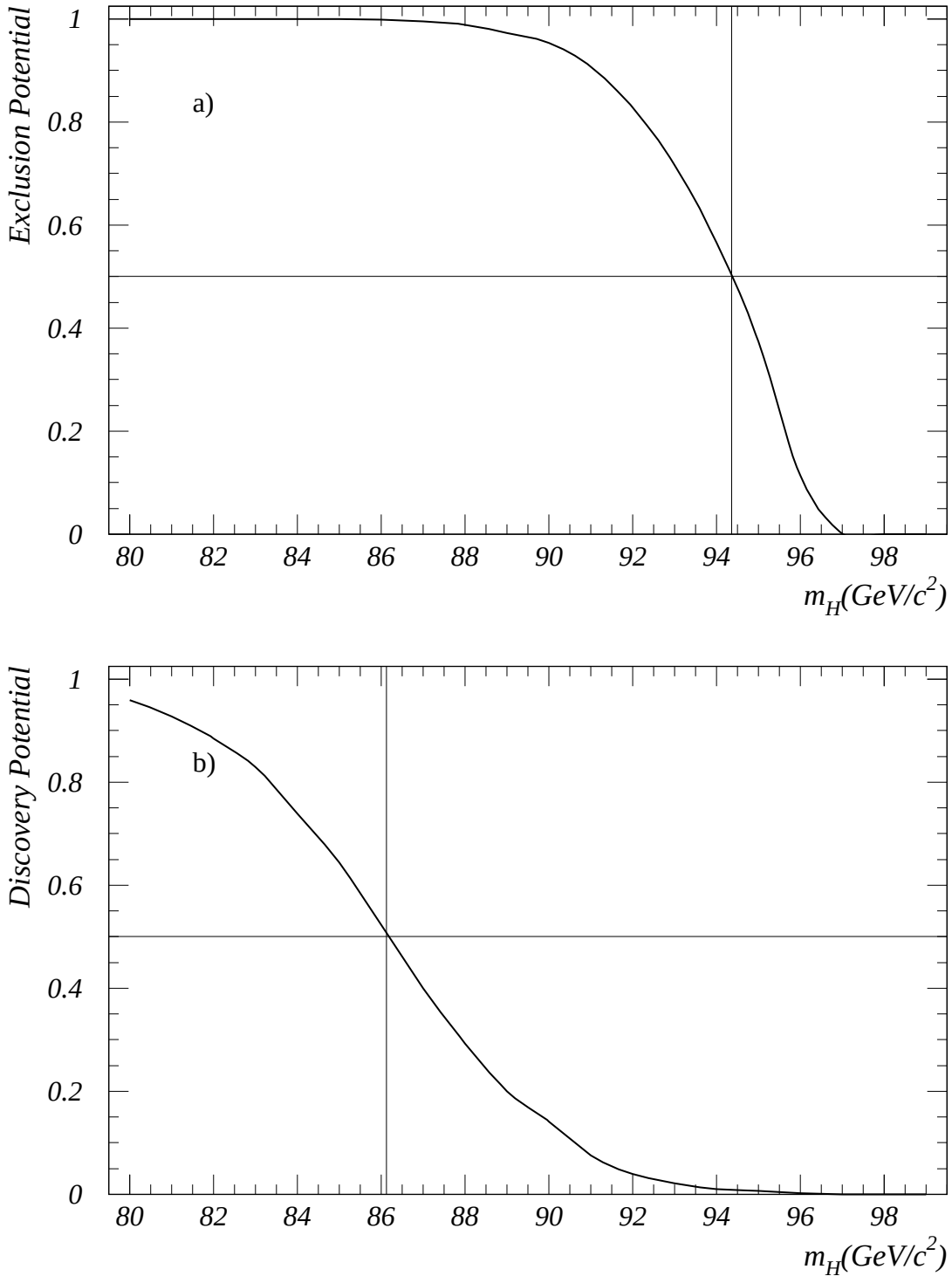

Figure 8: The probability for excluding the Higgs boson in background experiments (a) and the probability for performing a "5σ" discovery in signal experiment (b) versus the Higgs mass hypothesis m_{H} for 30pb^{-1} per experiment at $\sqrt{s}$=189 GeV. The vertical lines indicate the expected exclusion and discovery mass limits according to the definitions of the target exclusion and discovery potentials indicated by the horizontal lines.

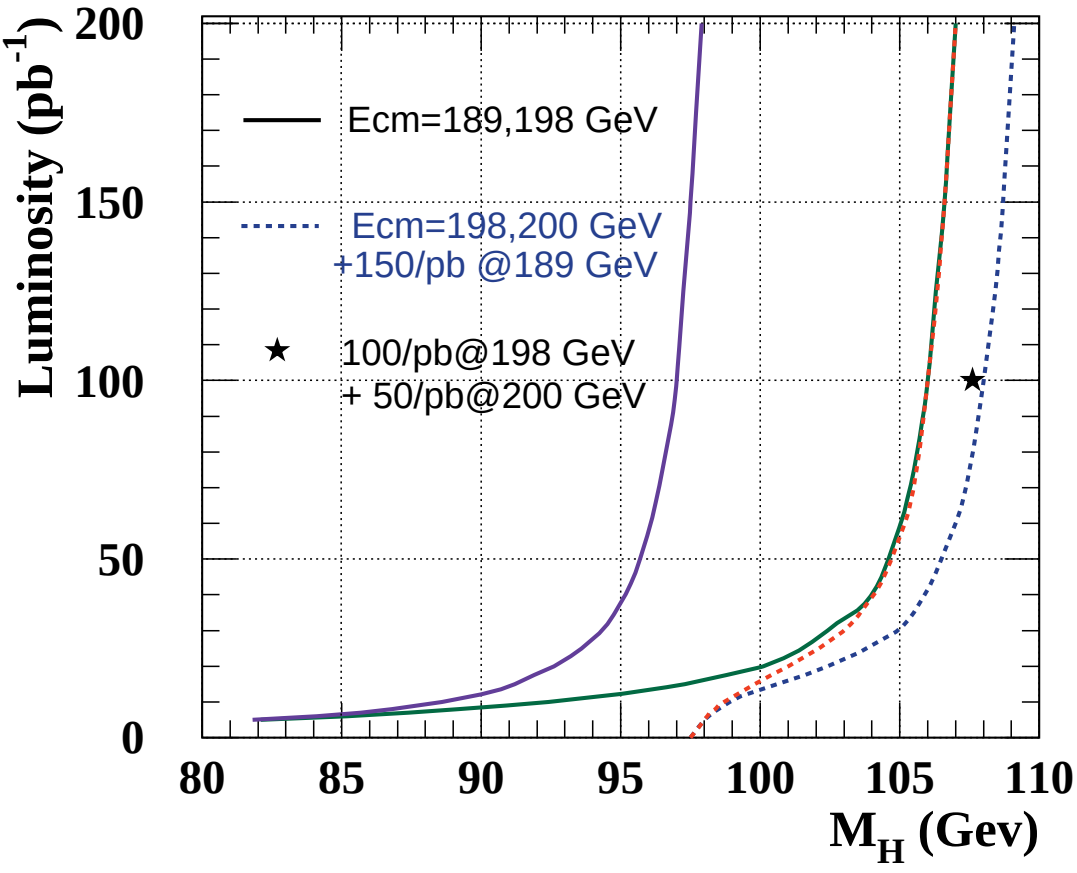

Figure 9: The minimum luminosity required in order to exclude the SM Higgs boson at the 95% Confidence Level at the indicated centre-of-mass energies of 189, 198 GeV and combining the luminosity collected at 198 and 200 GeV with 150 pb^{-1} collected at 189 GeV. The star on the right side indicates the exclusion sensitivity if one stops collecting data after 100 pb^{-1} at $\sqrt{s}$=198 GeV and upgrades to $\sqrt{s}$=200 GeV where additional 50 pb^{-1} are collected.

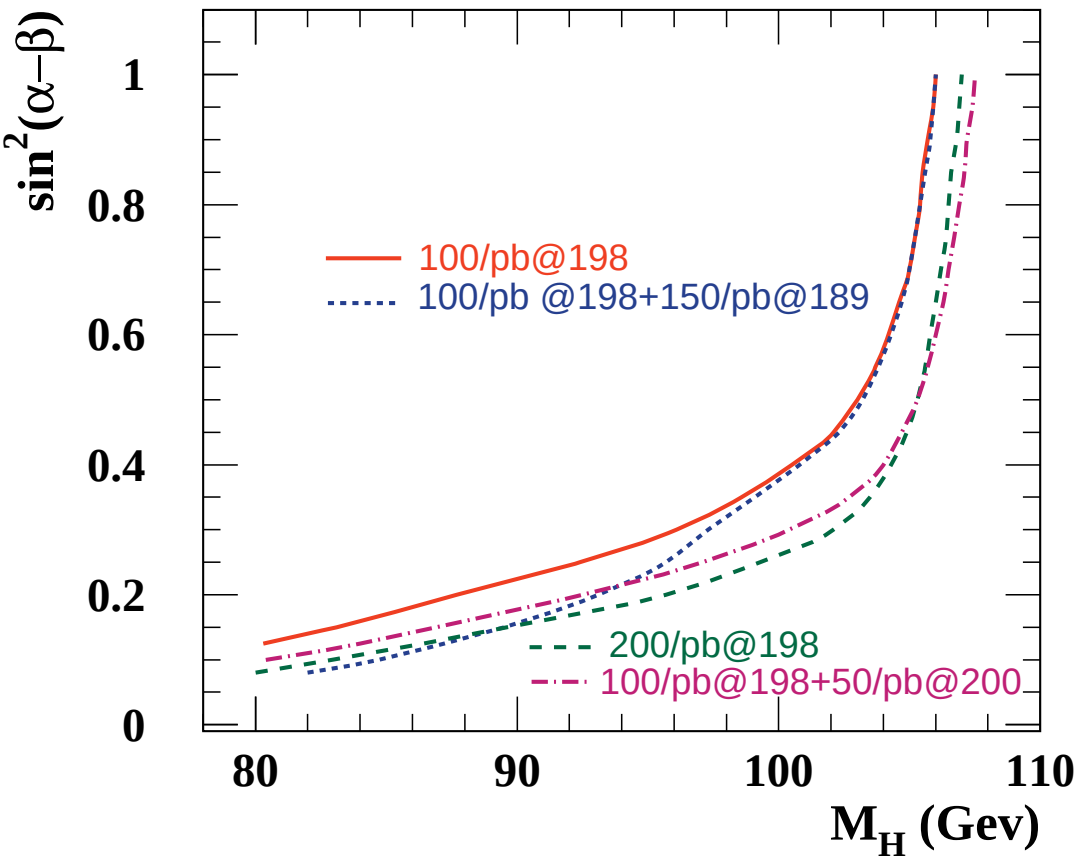

Figure 10: Prospective upper limits on $\sin^2(\beta-\alpha)$ as a function of the light MSSM Higgs mass. The curves are explained in the text.

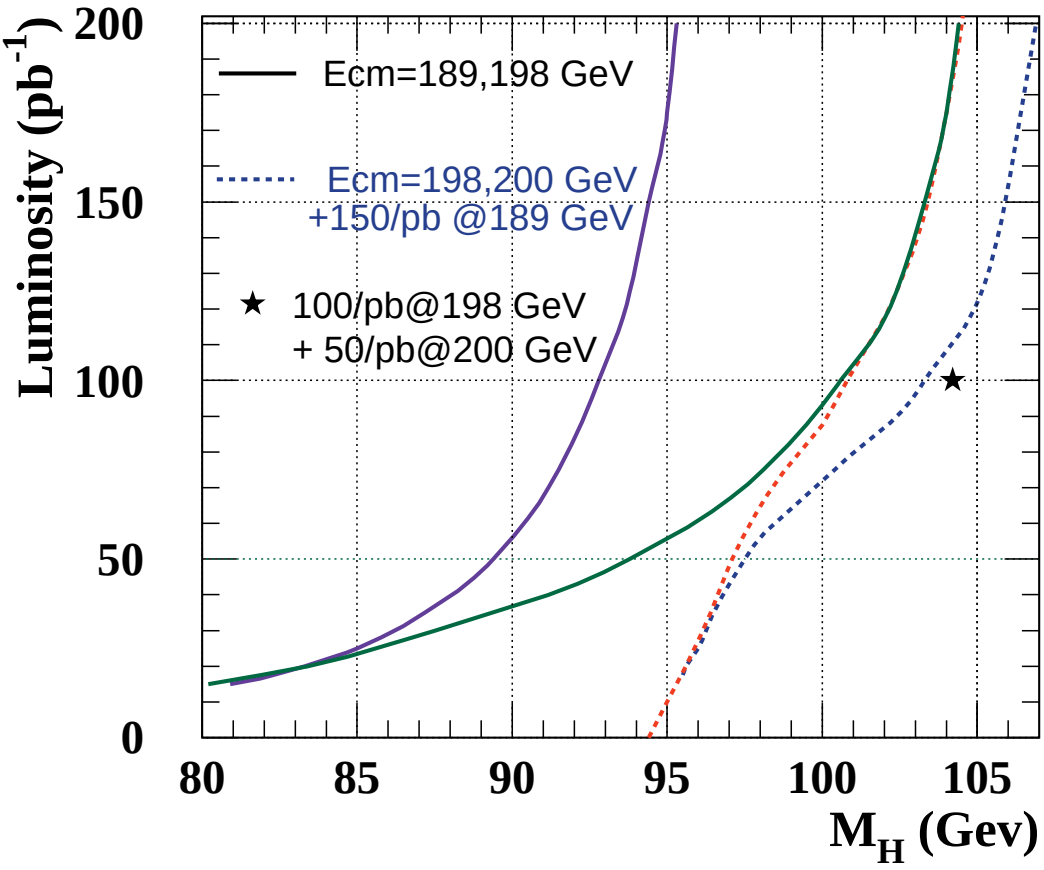

Figure 11: The minimum luminosity required in order to discover the SM Higgs boson at the 5σ level at the indicated centre-of-mass energies of 189, 198 GeV and combining the luminosity collected at 198 and 200 GeV with 150 pb^{-1} collected at 189 GeV. The star on the right side indicates the discovery sensitivity if one stops collecting data after 100 pb^{-1} at $\sqrt{s}$=198 GeV and upgrades to $\sqrt{s}$=200 GeV where additional 50 pb^{-1} are collected.